THE JOURNAL OF BIOLOGICAL CHEMISTRY VOL. 282, NO. 51, pp. 36820–36828, December 21, 2007

Identification of *in Vivo* Phosphorylation Sites and Their Functional Significance in the Sodium Iodide Symporter*

Received for publication, August 15, 2007, and in revised form, September 26, 2007 Published, JBC Papers in Press, October 3, 2007, DOI 10.1074/jbc.M706817200

Douangsone D. Vadysirisack[‡§], Eric S.-W. Chen[¶], Zhaoxia Zhang[§‖], Ming-Daw Tsai[¶], Geen-Dong Chang[**], and Sissy M. Jhiang[‡§‖‡‡1]

From the [‡]Integrated Biomedical Science Graduate Program, the [‖]Ohio State Biochemistry Program, and the Departments of [§]Physiology and Cell Biology and [‡‡]Internal Medicine, Ohio State University, Columbus, Ohio 43210, the [¶]Genomics Research Center, Academia Sinica, Taipei 115, Taiwan, and the [**]Graduate Institute of Biochemical Sciences, National Taiwan University, Taipei 106, Taiwan

The Na^+/I^- symporter (NIS)-mediated iodide uptake activity is the basis for targeted radioiodide ablation of thyroid cancers. Although it has been shown that NIS protein is phosphorylated, neither the *in vivo* phosphorylation sites nor their functional significance has been reported. In this study, Ser-43, Thr-49, Ser-227, Thr-577, and Ser-581 were identified as *in vivo* NIS phosphorylation sites by mass spectrometry. Kinetic analysis of NIS mutants of the corresponding phosphorylated amino acid residue indicated that the velocity of iodide transport of NIS is modulated by the phosphorylation status of Ser-43 and Ser-581. We also found that the phosphorylation status of Thr-577 may be important for NIS protein stability and that the phosphorylation status of Ser-227 is functionally silent. Thr-49 appears to be critical for proper local structure/conformation of NIS because mutation of Thr-49 to alanine, aspartic acid, or serine results in reduced NIS activity without alterations in total or cell surface NIS protein levels. Taken together, we showed that NIS protein levels and functional activity could be modulated by phosphorylation through distinct mechanisms.

The Na^+/I^- symporter (NIS)[2] is an intrinsic membrane glycoprotein most commonly studied in context with the thyroid gland, where it facilitates active transport of dietary iodide from the systemic circulation into thyroid follicular cells for synthesis of thyroid hormones triiodothyronine and thyroxine. The current topology of NIS proposes that it contains 13 putative transmembrane segments with an extracellular amino terminus and an intracellular carboxyl terminus. Electrophysiological studies demonstrate that NIS cotransports two Na^+ ions along with one I^- ion into cells (1). The iodide-concentrating activity of NIS serves as the basis for the clinical use of radioiodide in the detection and targeted destruction of differentiated thyroid carcinomas and their metastases. However, NIS expression and function are generally low or absent in patients with advanced thyroid cancer, consequently rendering radioiodide therapy ineffective. Therefore, investigations of the regulatory mechanisms of NIS expression and functional activity are of clinical significance.

It has been shown in cultured thyroid cells that deprivation of thyroid-stimulating hormone resulted in reduction of NIS protein half-life from 5 to 3 days and redistribution of NIS protein from the cell surface to intracellular compartments (2). Recently, we found that the velocity of iodide transport was decreased by MEK inhibition, which accounted for the discordance between cell surface NIS levels and NIS-mediated radioiodide uptake (RAIU) activity in PD98059-treated cells (3). In addition, some thyroid tumors had NIS protein detected exclusively at intracellular compartments, preventing these tumors from benefiting from NIS-mediated radioiodide imaging/therapy because of lack of cell surface NIS (4, 5). Taken together, these studies indicate that NIS protein levels, cell surface localization, and functional activity can be modulated at the post-translational level. However, the underlying mechanisms of these modulations are currently unknown. Because it has been reported that NIS is a phosphoprotein (2), we hypothesize that NIS expression, subcellular trafficking, and/or activity may be modulated by phosphorylation status.

In this study, we report the identification of five *in vivo* phosphorylated amino acid residues in NIS by mass spectrometry analysis. We examined the roles of these phosphorylated amino acid residues in total and cell surface NIS protein levels as well as functional activity by site-directed mutagenesis. We found that phosphorylated residues Ser-43 and Ser-581 modulate the velocity of iodide transport of NIS, that phosphorylated residue Thr-577 may be important for NIS protein stability, and that NIS cell surface trafficking is not affected by the phosphorylation status of these five amino acid residues.

EXPERIMENTAL PROCEDURES

Cell Culture and Reagents—HEK293 human embryonic kidney cells were maintained in Dulbecco's modified Eagle's medium with 10% fetal bovine serum (Invitrogen) supplemented with 1% penicillin/streptomycin. Transfection of

* This work was supported in part by NIBIB Grant 1 R01 EB001876 from the National Institutes of Health (to S. M. J.) and by National Health Research Institutes Grant EX95-9508NI (to M.-D. T.). The costs of publication of this article were defrayed in part by the payment of page charges. This article must therefore be hereby marked "*advertisement*" in accordance with 18 U.S.C. Section 1734 solely to indicate this fact.

[1] To whom correspondence should be addressed: Ohio State University, 304 Hamilton Hall, 1645 Neil Ave., Columbus, OH 43210. Tel.: 614-292-4312; Fax: 614-292-4888; E-mail: jhiang.1@osu.edu.

[2] The abbreviations used are: NIS, Na^+/I^- symporter; MAPK, mitogen-activated protein kinase; MEK, mitogen-activated protein kinase/extracellular signal-regulated kinase kinase; RAIU, radioiodide uptake; MS, mass spectrometry; LC-MS/MS, liquid chromatography-tandem mass spectrometry; LTQ, linear quadrupole ion trap; FT, Fourier transform; hNIS, human NIS; rNIS, rat NIS.

HEK293 cells was performed using FuGENE 6 (Roche Applied Science).

Immunoprecipitation of FLAGrNIS—HEK293 cells were transfected with plasmid encoding rat NIS tagged with a FLAG epitope at its extracellular N terminus (FLAGrNIS) in pcDNA3 vector (6). Cells were lysed with lysis buffer containing 50 mM Tris-HCl, pH 7.4, 150 mM NaCl, 1% Igepal, 1 mM phenylmethylsulfonyl fluoride, 10 μg/ml aprotinin, 10 μg/ml leupeptin, 50 mM NaF, and 5 mM sodium orthovandate. Whole cell extract (5 mg) was precleared with mouse IgG-agarose beads (Sigma) for 1 h at 4 °C. The clarified supernatant was then incubated with anti-FLAG antibody M2-conjugated agarose beads (Sigma) for 2 h at 4 °C. The beads were washed four times, and proteins were eluted using 250 ng/μl 3X FLAG peptide (Sigma) in lysis buffer for 30 min at 4 °C. The eluted proteins were separated on 10% SDS-polyacrylamide gels. Gels were subjected to either Coomassie Blue staining using GelCode blue stain reagent (Pierce) or electrotransfer followed by Western blot analysis. Gel slices corresponding to FLAGrNIS as detected by Western blot analysis were excised, and in-gel proteolytic digestions were performed.

In-gel Digestion and Phosphopeptide Enrichment—Gel slices were subjected to in-gel reduction with 10 mM dithiothreitol (GE Healthcare) for 1 h at 56 °C, followed by alkylation with 55 mM iodoacetamide (Sigma) for 45 min at room temperature in the dark. Gel slices were washed and then incubated with sequence-grade trypsin solution (Promega) and 25 mM ammonium bicarbonate overnight at 37 °C. Tryptic digestion solution was collected, and peptides were extracted twice with 60% acetonitrile and 1% trifluoroacetic acid (Riedel-de Haën). The peptide extracts were dried in a SpeedVac (Thermo Electron) to remove organic solvent and partial salts of ammonium bicarbonate. 20% of the dry peptide extracts were analyzed by liquid chromatography-tandem mass spectrometry (LC-MS/MS), and 80% of the dry peptides were processed with a phosphopeptide capturing kit (MB-IMAC Fe, Bruker Daltonics) followed by LC-MS/MS analysis.

LC-MS/MS—Peptide nanoflow LC-MS/MS experiments were performed on a linear quadrupole ion trap Fourier transform (LTQ-FT) ion cyclotron resonance mass spectrometer (Thermo Electron) equipped with a nanoelectrospray ion source (New Objective), an Agilent 1100 Series binary high-performance liquid chromatography pump (Agilent Technologies), and a Famos autosampler (LC Packings). In-gel tryptic peptide mixtures were injected at a 9-μl/min flow rate to a self-packed precolumn (150 μm, inner diameter × 20 mm) with C_{18} reverse phase resin (Magic C_{18}AQ; particle size, 5 μm; pore size, 200 Å; Michrom Bioresources). Chromatographic separation of peptide mixtures was performed on a self-packed reversed phase C_{18} nanocolumn (75 μm, inner diameter × 30 cm) and an in-house prepared needle tip with an internal diameter of 3~5 μm. Separation was achieved by using 0.1% formic acid in water as mobile phase A and 0.1% formic acid in 80% acetonitrile as mobile phase B and applying a linear gradient from 10 to 40% mobile phase B during a 60-min LC-MS/MS analysis at a split flow rate of around 300 nl/min. Electrospray voltage was applied at 2.5 kV, and capillary temperature was set at 200 °C. The mass spectrometer was operated in two different data-dependent survey scans based on phosphoric acid neutral loss trigger MS3 and speed. With phosphoric acid neutral loss trigger MS3 mode, a scan cycle was initiated with a full-scan survey mass spectrometry (MS; m/z 300–1800) experiment performed with the FT ion cyclotron resonance mass spectrometer. The three most abundant ions detected in this scan were subjected to an FT ion cyclotron resonance selected ion monitoring (±2.5 m/z) scan followed by a MS/MS experiment in a LTQ mass spectrometer with phosphoric acid neutral loss trigger MS3. Ion accumulation of auto gain control target and maximal ion accumulation time for MS, selected ion monitoring, and MS/MS were as follows: 1×10^6 ions, 1000 ms; 5×10^4 ions, 500 ms; and 5×10^4 ions, 500 ms, respectively. Resolution of full MS and selected ion monitoring was set as 2.5×10^4 and 5×10^4, respectively. MS/MS spectra were collected in the LTQ mass spectrometer, and ions were selected (±3 m/z) for MS/MS when their intensity exceeded a minimum threshold of 1000 counts. Singly charged ions were rejected by MS/MS. The normalized collision energy was set to 25%, and one microscan was acquired per spectrum. Ions subjected to MS/MS were excluded from further sequencing for 120 s (repeat count 2). Another scan cycle without MS3 was initiated with a full-scan survey MS experiment (m/z 320–1800; auto gain control target, 1×10^6 ions; resolution, 1×10^5; maximum ion accumulation time, 1000 ms) performed with the FT ion cyclotron resonance mass spectrometer followed by MS/MS experiments on the 10 most abundant ions detected in the full-MS scan. Except for neutral loss trigger MS3, the MS/MS setting was identical to the other mode setting.

Peptide Assignments—The DTA files were outputted with Bioworks software (mass range, 640–5400 Da; threshold, absolute 100; precursor tolerance, 50 ppm; 0 group scan; 1 minimum group count; 5 minimum ion counts; Thermo Electron) and merged into a single file for further Mascot (version 2.1, Matrix Science) MS/MS ion searching in the Rattus database (SWISS-PROT). Peptide tolerances in MS and MS/MS modes for LTQ-FT were 5 ppm and 0.8 Da, respectively, in selected ion monitoring mode and 10 ppm and 0.8 Da in only full-scan mode. Two missed cleavages by trypsin were allowed. Only peptides with clear mass spectra with a Mascot score of >95% reliability were considered in this study. Ambiguous phosphorylation sites from Mascot scoring were further evaluated with post-translational modification scoring (7) using MSQuant software.

Site-directed Mutagenesis—FLAGrNIS or FLAGhNIS (plasmid encoding human NIS tagged with a FLAG epitope at its extracellular N terminus in pcDNA3 vector) served as a template. FLAGrNIS or FLAGhNIS phospho-defective or phospho-mimicking mutant constructs were generated using the QuikChange site-directed mutagenesis kit (Strategene) according to the manufacturer's instructions. The nucleotide sequences of all cDNA constructs were verified by automated DNA sequencing.

Radioiodide Uptake Assay—Steady-state radioiodide accumulation was determined as follows. Cells were incubated with 2 μCi of $Na^{125}I$ in 5 μM nonradioactive NaI at 37 °C with 5% CO_2 for 30 min, a time point that reflects iodide accumulation in equilibrium. Cells were washed twice with cold Hanks' bal-

anced salt solution and then lysed with cold 95% ethanol for 20 min at room temperature. Cell lysate was collected, and radioactivity was counted by a γ counter (Packard Instruments). Experiments were performed in triplicate.

Iodide-dependent Kinetic Analysis—Cells were incubated for 2 min with varying concentrations of NaI (from 0 to 600 μM) containing $Na^{125}I$ of a specific activity of 80mCi/mmol. The amounts of accumulated iodide were measured as described above. The K_m and V_{max} values for I^- were derived from the fitted Michaelis-Menten equation according to the Eadie-Hofstee plot. Experiments were performed in triplicate.

Western Blot Analysis—Cells were lysed in lysis buffer containing 50 mM Tris, pH 7.5, 150 mM NaCl, 5 mM EDTA, 1% Triton X-100, 1 mM phenylmethylsulfonyl fluoride, 10 μg/ml aprotinin, and 10 μg/ml leupeptin. Protein concentrations were determined by Bradford assay (Bio-Rad). Proteins were subjected to 10% SDS-PAGE and transferred to a nitrocellulose membrane (Schleicher & Schuell). The membrane was blocked in buffer containing 10 mM Tris-HCl, pH 8.0, 150 mM NaCl, and 0.05% Tween 20 with 5% nonfat dry milk. Next, the membrane was incubated with mouse anti-FLAG monoclonal antibody M2 (Sigma, 1:1000 dilution) for 1 h at room temperature, followed by incubation with horseradish peroxidase-conjugated anti-mouse IgG (Cell Signaling, 1:4000 dilution) for 1 h at room temperature. The signal was detected by ECL detection reagent (Amersham Biosciences). To determine equal protein loading of total NIS proteins, the membrane was probed with mouse anti-β-actin monoclonal antibody (Abcam, 1:2000 dilution) followed by incubation with horseradish peroxidase-conjugated anti-mouse IgG. The signal intensities were measured densitometrically using NIH Image software.

Nonpermeabilized Flow Cytometry Analysis—To detect cell surface NIS protein levels, flow cytometric analysis was performed using nonpermeabilized cells that were incubated with either a mouse anti-FLAG monoclonal antibody M2 (Sigma, 1:50 dilution) or an isotype IgG mouse control (Sigma, 1:50 dilution) for 1 h at 4 °C followed by incubation with fluorescein isothiocyanate-conjugated goat anti-mouse IgG antibody (Sigma, 1:100 dilution) for 30 min at 4 °C. Cells were washed and then resuspended in fixative buffer (1% paraformaldehyde in phosphate-buffered saline) for analysis by a FACSCalibur flow cytofluorometer (BD Biosciences). The positive events region was gated at a fluorescence density that had $<1\%$ of cells with nonspecific fluorescence. Cell surface NIS levels were quantified by multiplying the percentage of cells by the mean fluorescence density in the gated region.

Statistical Analysis—Comparisons between groups were performed using the paired *t* test. A p value <0.05 was considered to be statistically significant.

RESULTS

Mass Spectrometry Identifies Five in Vivo Phosphorylated Amino Acid Residues in rNIS—Although it has been shown that NIS is a phosphoprotein (2), neither the phosphorylated amino acid residues nor the role of phosphorylation in NIS expression/activity has been reported. We first sought to directly identify *in vivo* phosphorylated amino acid residues in NIS using mass spectrometry. A heterologous expression system was employed to acquire sufficient amounts of immunopurified NIS protein for mass spectrometry analysis. We immunoprecipitated rat NIS tagged with a FLAG epitope at its extracellular N terminus (FLAGrNIS) from transfected HEK293 cells using anti-FLAG antibody M2 and subsequently conducted proteomic analysis. As shown in Fig. 1*A*, the resulting proteolytic digestion in combination with LC-MS/MS fragmentation provided extensive sequence coverage of NIS protein of about 76%. Without enrichment for phosphopeptides, Ser-227 was identified as a phosphorylated amino acid residue in NIS by LC-MS/MS analysis (Fig. 1*B*). Following enrichment for phosphopeptides by immobilized metal affinity chromatography, two additional phosphopeptides with four phosphorylated amino acid residues of NIS were identified. However, we found ambiguity between Thr-575 and Thr-577 of phosphopeptide EDTATTLEESLVK using the Mascot search engine. Accordingly, the ambiguity between Thr(P)-575 and Thr(P)-577 was evaluated by post-translational modification scoring using MSQuant software. The score of Thr(P)-577 was about twice the score of Thr(P)-575 after post-translational modification scoring. Differences in liquid chromatography retention times were used to distinguish between Ser(P)-43- and Thr(P)-49-containing phosphopeptides, as well as between Thr(P)-577- and Ser(P)-581-containing phosphopeptides. Based on the current proposed secondary structure of rNIS, the identified phosphorylated amino acid residues Ser-43, Thr-49, Thr-577 (or Thr-575), and Ser-581 are in the intracellular domains of NIS protein (Fig. 1*C*). However, Ser-227 is predicted to be in the extracellular domains of NIS protein, which is an unusual location for phosphorylation. Nonetheless, neutral loss of H_3PO_4 did occur in the MS/MS fragmentation, and the MS/MS fragmentation assignment of Ser(P)-227 from Mascot scoring was high. The estimated stoichiometry of Ser(P)-227 as measured by using the algorithm published by Wu *et al.* (8) was $6.65 \pm 0.8\%$. In summary, we successfully identified five *in vivo* phosphorylated amino acid residues in NIS protein by mass spectrometry.

Phosphorylation Status of Ser-43 and Ser-581 Modulates NIS Activity without Altering Total or Cell Surface NIS Protein Levels—To examine the functional importance of the identified phosphorylated amino acid residues, we generated NIS phospho-defective or phospho-mimicking mutants of the corresponding amino acid residue to evaluate NIS-mediated RAIU activity and total NIS protein levels as well as cell surface NIS levels in transfected HEK293 cells. Site-directed mutagenesis was performed to replace the selected phosphorylated serine/threonine residue in FLAGrNIS with either alanine or aspartic acid. As shown in the *left panel* of Fig. 2*A*, cells expressing NIS phospho-defective single mutants S43A, T49A, T577A, and S581A, but not S227A or T575A, had reduced NIS-mediated RAIU activity of $\sim$30–60% that of wild-type FLAGrNIS. Conversely, NIS phospho-mimicking single mutants S43D, T577D, and S581D had RAIU activity comparable with that of wild-type FLAGrNIS (Fig. 2*A*, *right panel*). These results suggest that the phosphorylation status of Ser-43, Thr-577, or Ser-581 modulates NIS activity. In comparison, both T49A and T49D mutations resulted in reduced RAIU activity of similar extent; thus the role of phosphorylation status of Thr-49 in

A.

```
  1 MEGAEAGARA TFCAWDYGVF ATMLLVSTGI GLMVGLARGG QRSADDFFTG
 51 GRQLAAVPVG LSLAASFMSA VQVLGVPAEA ARYGLKFLWM CAGQLLNSLL
101 TAFLFLPIFY RLGLTSTYQY LELRFSRAVR LCGTLQYLVA TMLYTGIVIY
151 APALILNQVT GLDIWASLLS TGIICTLYTT VGGMKAVVWT DVFQVVVMLV
201 GFWVILARGV ILLGGPRNVL SLAQNHSRIN LMDFDPDPRS RYTFWTFYVG
251 GTLVWLSMYG VNQAQVQRYV ACHTEGKAKL ALLVNQLGLF LIVASAACCG
301 IVMFVYYKDC DPLLTGRISA PDQYMPLLVL DIFEDLPGVP GLFLACAVSG
351 TLSTASTSIN AMAAVTVEDL IKPRMPGLAP RKLVFISKGL SFIYGSACLT
401 VAALSSLLGG GVLQGSFTVM GVISGPLLGA FTLGMLLPAC NTPGVLSGLA
451 AGLAVSLWVA VGATLYPPGE QTMGVLPTSA AGCTNDSVLL GPPGATNASN
501 GIPSSGMDTG RPALADTFYA ISYLYYGALG TLTTMLCGAL ISYLTGPTKR
551 SSLGPGLLWW DLARQTASVA PKEDTATLEE SLVKGPEDIP AVTKKPPGLK
601 PGAETHPLYL GHDVETNL
```

B.

Phosphorylation of amino acid residues in rNIS

Peptide sequence	Phosphorylation site	MW (observed)	MW (theoretical)	ΔM	
SADDFFTGGR	Ser 43	1151.4298	1151.4284	1.40 mDa	1.21 ppm
SADDFF**T**GGR	Thr 49	1151.4291	1151.4284	0.60 mDa	0.52 ppm
NVLSLAQNH**S**R	Ser 227	1317.6238	1317.6190	4.70 mDa	3.56 ppm
EDTA**T**LEESLVK	Thr 577	1413.6328	1413.6276	5.20 mDa	3.68 ppm
EDTATLEE**S**LVK	Ser 581	1413.6283	1413.6276	0.70 mDa	0.50 ppm

C.

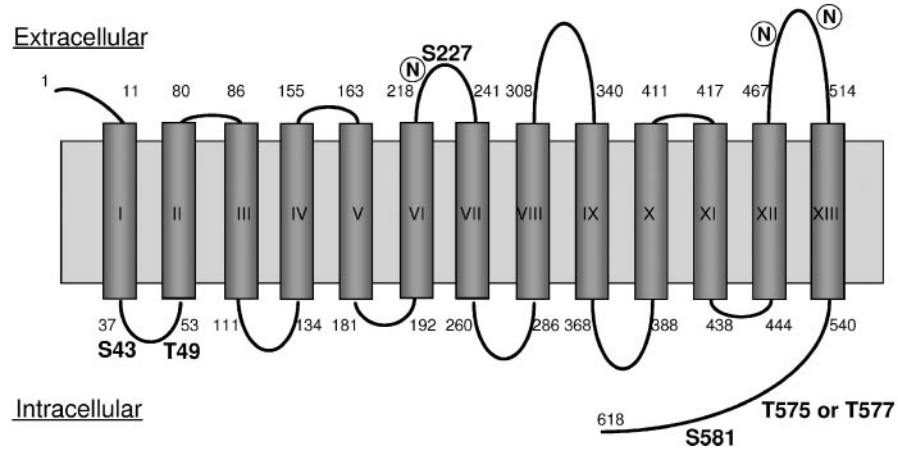

FIGURE 1. ***In vivo* phosphorylation of amino acid residues in rNIS.** *A*, *in vivo* phosphorylation of amino acid residues Ser-43, Thr-49, Ser-227, Thr-575 or Thr-577, and Ser-581 in rNIS was identified by mass spectrometry. Sequence coverage of 76% was achieved and is indicated in *black*. Phosphorylation sites are indicated by *underlined letters*. Rat NIS tagged with a FLAG epitope at its extracellular N terminus was immunoprecipitated from transfected HEK293 cells using anti-FLAG antibody M2 and run on a 10% SDS-polyacrylamide gel, which was then stained with Coomassie Blue. Gel slices corresponding to FLAGrNIS were excised and subjected to in-gel proteolytic digestion. Phosphopeptides were enriched by immobilized metal affinity chromatography, and the resulting peptide extracts were analyzed by LC-MS/MS. *B*, three phosphopeptides with five phosphorylated amino acid residues of NIS were identified. The phosphopeptides were identified by the difference in observed mass values due to the presence of phosphate moieties compared with theoretical mass values calculated from known amino acid sequences. Mass accuracy of peptide masses was <10 ppm. *C*, the schematic diagram shows the predicted secondary structure of rNIS with the locations of the identified phosphorylated amino acid residues and putative *N*-linked glycosylation sites.

NIS activity is uncertain. Consistent with the prediction of proteomic analysis, T577A, but not T575A, resulted in reduced RAIU activity.

In Fig. 2*B*, we show that total NIS protein levels were not different among cells expressing wild-type FLAGrNIS or NIS phospho-defective or phospho-mimicking mutants of Ser-43, Thr-49, or Ser-581 with the exception of cells expressing T577A. Whereas mutation to T577A resulted in reduced total NIS protein levels, mutation to T577D resulted in total NIS protein levels comparable with those of wild-type FLAGrNIS. These results suggest that the phosphorylation status of Thr-577 may alter NIS protein stability.

As NIS-mediated RAIU activity is determined by NIS expression at the cell surface, we next examined cell surface NIS levels by flow cytometric analysis in nonpermeabilized cells expressing NIS phospho-defective or phospho-mimicking single mutants. Consistent with the results of total NIS protein levels, cell surface NIS levels were comparable among cells expressing NIS phospho-defective or phospho-mimicking mutants of Ser-43, Thr-49, or Ser-581, except for T577A (Fig. 2*C*). As summarized in Fig. 2*D*, we found that the phosphorylation status of Ser-43 and Ser-581 modulates NIS activity without notable changes to total or cell surface NIS protein levels.

The Effects of Ser(P)-43 and Ser(P)-581 on NIS Activity Are Additive—To investigate whether phosphorylation of both amino acid residues Ser-43 and Ser-581 is important to confer optimal NIS activity, we generated NIS phospho-defective or phospho-mimicking double mutants at the two corresponding serine residues and examined NIS-mediated RAIU activity and NIS protein levels. As shown in Fig. 3*A*, NIS double mutants S43A/S581A, S43A/S581D, and S43D/S581A had reduced RAIU activity of about 40, 60, and 60%, respectively, compared with that of wild-type FLAGrNIS. These results suggest that the effects of Ser(P)-43 and Ser(P)-581 on NIS activity are additive. Indeed, S43A/S581D and S43D/S581A mutants had a similar extent of reduced RAIU activity compared with S43A and S581A mutants (Fig. 3*A* *versus* Fig. 2*A*), as the single mutants S43A and S581A could have Ser-581 and Ser-43, respectively, phosphorylated. In addition, NIS double mutant S43D/S581D had RAIU activity comparable with that of S43D, S581D, or wild-type FLAGrNIS (Fig. 3*A* *versus* Fig. 2*A*). As shown in Fig. 3, *B* and *C*, we observed no difference in total NIS protein levels or cell surface NIS levels among all four NIS double mutants of Ser-43, Ser-581, and wild-type FLAGrNIS. As summarized in Fig. 3*D*, phosphorylation of either Ser-43 or Ser-581 alone does not achieve optimal NIS activity.

Threonine Residue at Position 49 Provides an Important Structural Constraint for Optimal NIS Activity—To further examine whether structural geometry or phosphorylation sta-

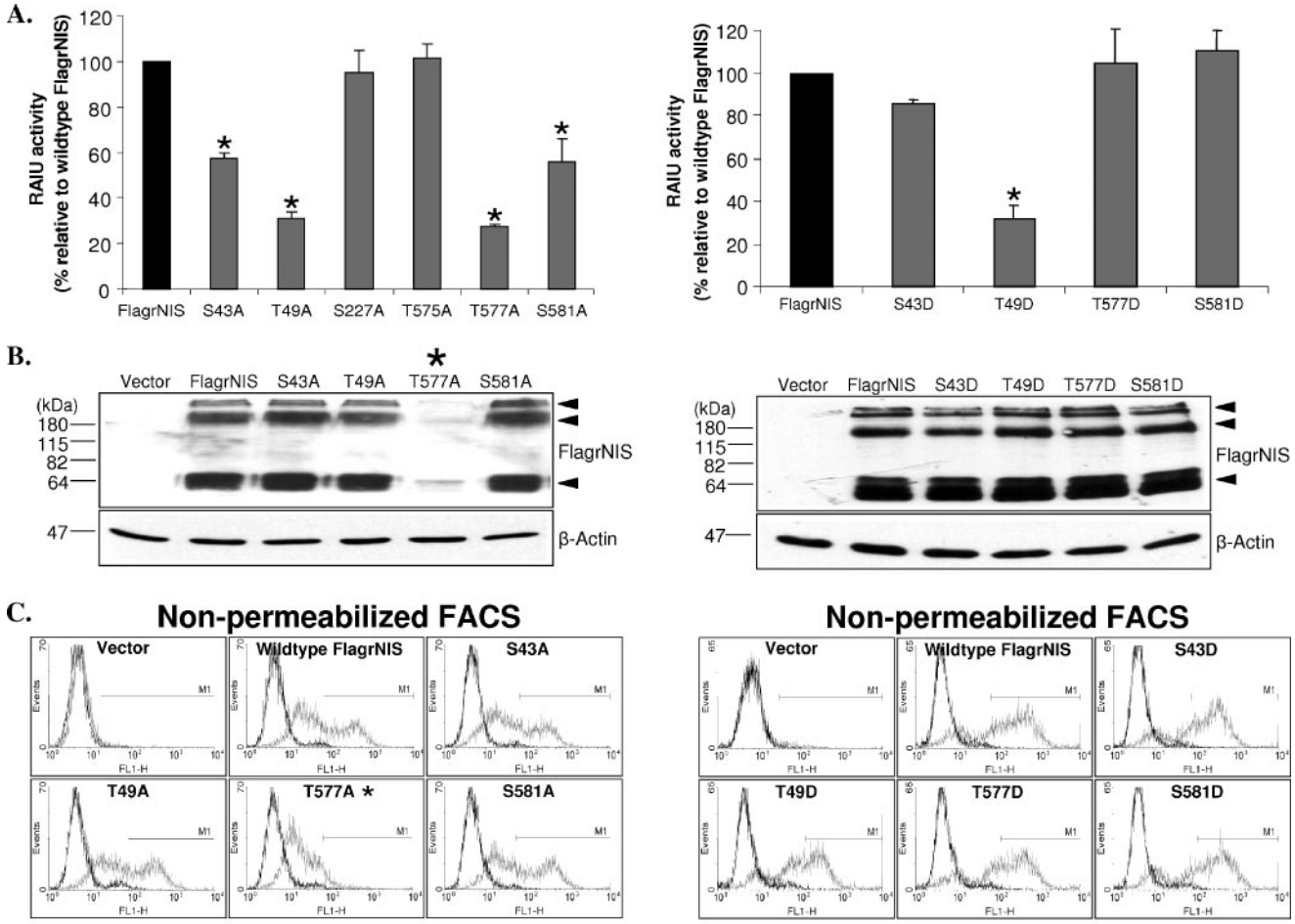

D.

	S43		T49		T577		S581	
	A	D	A	D	A	D	A	D
RAIU	↓	≈	↓	↓	↓	≈	↓	≈
Total NIS	≈	≈	≈	≈	↓	≈	≈	≈
Cell surface NIS	≈	≈	≈	≈	↓	≈	≈	≈

FIGURE 2. **Phospho-defective and phospho-mimicking mutations of Ser-43 or Ser-581 modulate NIS activity without affecting total or cell surface NIS protein levels.** *Asterisks* denote statistically significant difference in comparison with cells expressing wild-type FLAGrNIS ($p < 0.05$). *A*, NIS-mediated RAIU activity in HEK293 cells expressing FLAGrNIS phospho-defective mutant S43A, T49A, T577A, or S581A was reduced in comparison with cells expressing wild-type FLAGrNIS, whereas RAIU activity in cells expressing FLAGrNIS phospho-mimicking mutant S43D, T577D, or S581D was comparable with that in cells expressing wild-type FLAGrNIS. However, both T49A and T49D mutations resulted in reduced RAIU activity. The results represent the mean ± S.D. of three independent experiments performed in triplicate. *B*, Western blot analysis showed that total NIS protein levels were similar between cells expressing wild-type FLAGrNIS and cells expressing FLAGrNIS phospho-defective or phospho-mimicking mutants, except cells expressing T577A. Anti-FLAG antibody M2 was used to probe for total FLAGrNIS protein, whereas anti-β-actin antibody was used to monitor equal loading of samples. Please note that three immunoreactive bands were detected in cells expressing FLAGrNIS. The band around 64 kDa corresponds to partially glycosylated NIS protein, whereas the two immunoreactive bands around and above 180 kDa may represent dimeric/oligomeric forms of fully glycosylated NIS (~90 kDa) in HEK293 cells. The results are representative of three independent experiments. Densitometry analysis was performed to determine the -fold change of total NIS normalized with β-actin. *C*, flow cytometric analysis of nonpermeabilized cells demonstrated that cell surface NIS levels were comparable among cells except cells expressing T577A. Cells were incubated with anti-FLAG antibody M2 (*gray lines*) or with an isotype mouse IgG control (*black lines*) followed by fluorescein isothiocyanate-labeled anti-mouse secondary antibody. The results are representative of three independent experiments. Cell surface NIS levels were quantified by multiplying the percentage of cells by the mean fluorescence density in the gated region. *D*, the table summarizes the results of activity and protein levels of NIS phospho-defective and phospho-mimicking single mutants.

tus of Thr-49 is important for optimal NIS activity, we generated the T49S mutant and evaluated NIS-mediated RAIU activity as well as protein levels. We found that the T49S mutant had a similar extent of reduced RAIU activity (Fig. 4*A*) compared with either the T49A or T49D mutant (Fig. 2*A*). As serine represents a phospho-group-accepting amino acid residue that often is used to substitute for threonine, we concluded that the phosphorylation status of Thr-49 might not play an important role for optimal NIS activity. Instead, the structural geometry provided by the threonine residue at position 49 is important to achieve proper local structure/conformation of NIS protein for optimal activity. In comparison, we found that the S43T mutant had RAIU activity comparable with that of the S43D mutant as well as wild-type FLAGrNIS. These results suggest that the

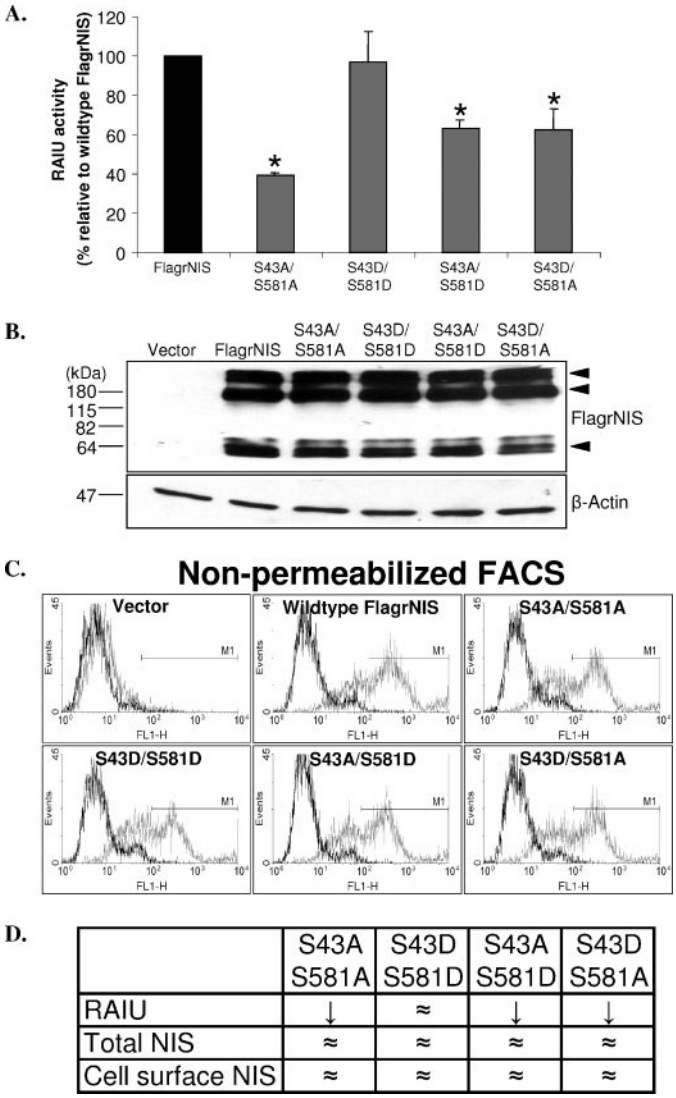

D.

	S43A S581A	S43D S581D	S43A S581D	S43D S581A
RAIU	↓	≈	↓	↓
Total NIS	≈	≈	≈	≈
Cell surface NIS	≈	≈	≈	≈

FIGURE 3. **The effects of Ser(P)-43 and Ser(P)-581 on NIS activity are additive.** *Asterisks* denote statistically significant difference in comparison with cells expressing wild-type FLAGrNIS ($p < 0.05$). *A*, NIS-mediated RAIU activity in HEK293 cells expressing FLAGrNIS double mutant S43A/S581A, S43A/S581D, or S43D/S581A was reduced, whereas RAIU activity in cells expressing S43D/S581D was comparable with that in cells expressing wild-type FLAGrNIS. The results represent the mean ± S.D. of three independent experiments performed in triplicate. *B*, Western blot analysis showed that total NIS protein levels were similar between cells expressing FLAGrNIS double mutants and wild-type FLAGrNIS. Anti-FLAG antibody M2 was used to probe for total FLAGrNIS protein, whereas anti-β-actin antibody was used to monitor equal loading of samples. The results are representative of three independent experiments. Densitometry analysis was performed to determine the -fold change of total NIS normalized with β-actin. *C*, flow cytometric analysis of nonpermeabilized cells demonstrated that cell surface NIS levels were comparable among all cells. Cells were incubated with anti-FLAG antibody M2 (*gray lines*) or with the isotype mouse IgG control (*black lines*) followed by fluorescein isothiocyanate-labeled anti-mouse secondary antibody. The results are representative of three independent experiments. Cell surface NIS levels were quantified by multiplying the percentage of cells by the mean fluorescence density in the gated region. *D*, the table summarizes the results of activity and protein levels of NIS phospho-defective and phospho-mimicking double mutants at amino acid residues Ser-43 and Ser-581.

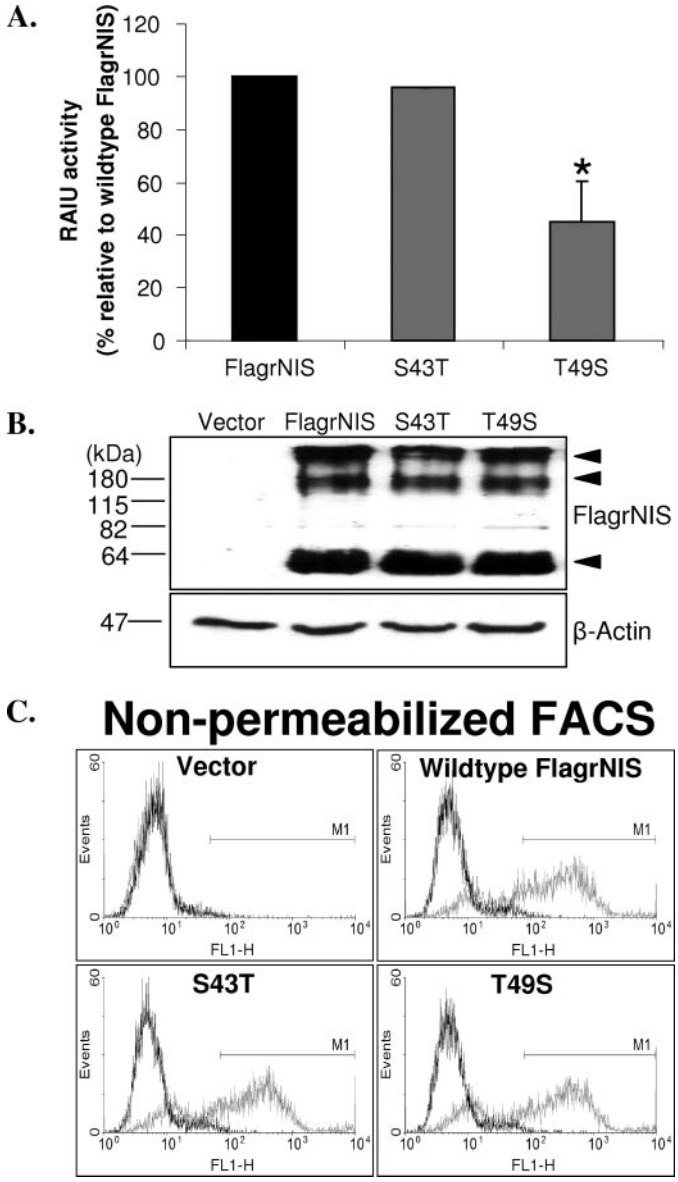

FIGURE 4. **Structural geometry, rather than phosphorylation status, of threonine residue at position 49 is important for optimal NIS activity.** The *asterisk* denotes statistically significant difference in comparison with cells expressing wild-type FLAGrNIS ($p < 0.05$). *A*, NIS-mediated RAIU activity in HEK293 cells expressing FLAGrNIS mutant T49S, but not S43T, was reduced in comparison with cells expressing wild-type FLAGrNIS. The results represent the mean ± S.D. of three independent experiments performed in triplicate. *B*, Western blot analysis showed that total NIS protein levels were similar among cells expressing FLAGrNIS S43T, T49S, or wild-type FLAGrNIS. Anti-FLAG antibody M2 was used to probe for total FLAGrNIS protein, whereas anti-β-actin antibody was used to monitor equal loading of samples. The results are representative of three independent experiments. Densitometry analysis was performed to determine the -fold change of total NIS normalized with β-actin. *C*, flow cytometric analysis of nonpermeabilized cells demonstrated that cell surface NIS levels were comparable among all cells. Cells were incubated with anti-FLAG antibody M2 (*gray lines*) or with isotype mouse IgG control (*black lines*) followed by fluorescein isothiocyanate-labeled anti-mouse secondary antibody. The results are representative of three independent experiments. Cell surface NIS levels were quantified by multiplying the percentage of cells by the mean fluorescence density in the gated region.

phosphorylation status of Ser-43 modulates NIS functional activity. Total NIS protein levels (Fig. 4*B*) and cell surface NIS protein levels (Fig. 4*C*) of S43T and T49S mutants were comparable with those of wild-type FLAGrNIS.

Functional Importance of Phosphorylation Status of Ser-43 Is Conserved between Rat and Human Species—Sequence analysis has shown that human NIS protein exhibits 84% identity and 92% similarity to rat NIS protein (9). Three of the five identified

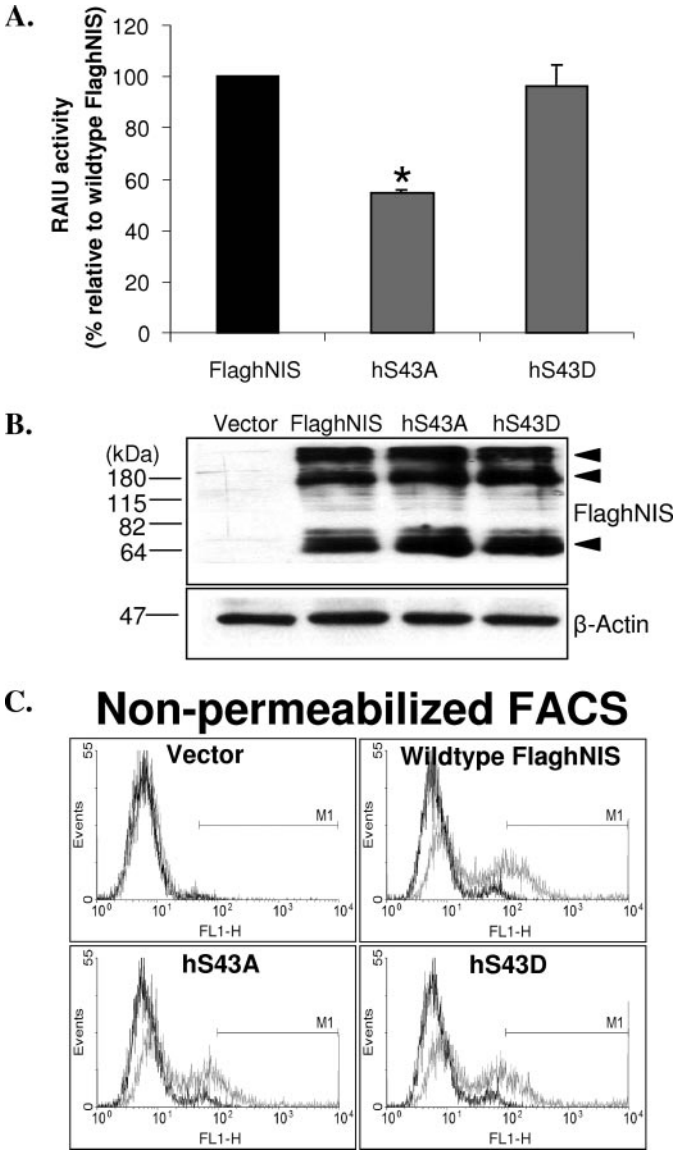

FIGURE 5. **Functional importance of phosphorylation status of Ser-43 is conserved between rat and human species.** The *asterisk* denotes a statistically significant difference in comparison with cells expressing wild-type FLAGhNIS ($p < 0.05$). *A*, NIS-mediated RAIU activity in HEK293 cells expressing FLAGhNIS S43D (*hS43D*), but not S43A (*hS43A*), was comparable with that in cells expressing wild-type FLAGhNIS. The results represent the mean ± S.D. of three independent experiments performed in triplicate. *B*, Western blot analysis showed that total hNIS protein levels were similar among cells expressing S43A, S43D, or wild-type FLAGhNIS. Anti-FLAG antibody M2 was used to probe for total FLAGhNIS protein, whereas anti-β-actin antibody was used to monitor equal loading of samples. The results are representative of three independent experiments. Densitometry analysis was performed to determine the -fold change of total NIS normalized with β-actin. *C*, flow cytometric analysis of nonpermeabilized cells demonstrated that cell surface hNIS levels were comparable among all cells. Cells were incubated with anti-FLAG antibody M2 (*gray lines*) or with an isotype mouse IgG control (*black lines*) followed by fluorescein isothiocyanate-labeled anti-mouse secondary antibody. The results are representative of three independent experiments. Cell surface NIS levels were quantified by multiplying the percentage of cells by the mean fluorescence density in the gated region.

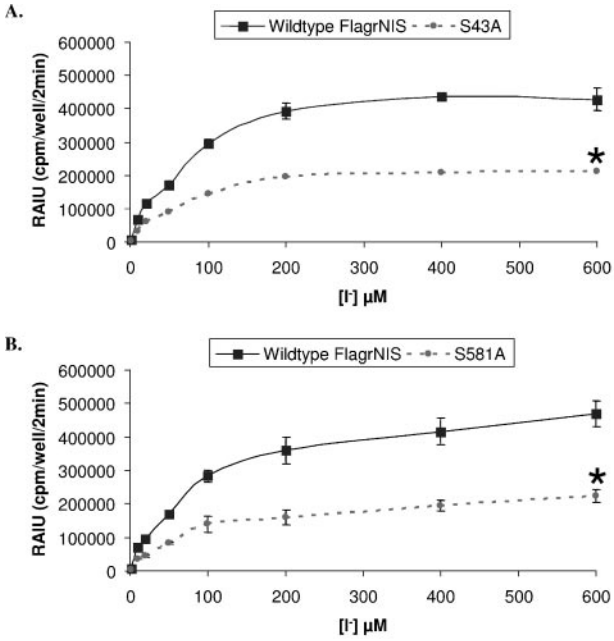

C.

	Vmax (% relative)
wildtype	100
S43A	36 ± 11.7
S581A	59 ± 12.6

	Km (μM)
wildtype	63 ± 4.8
S43A	53 ± 7.2
S581A	63 ± 1.0

FIGURE 6. **Phospho-defective mutation of either Ser-43 or Ser-581 reduces NIS V_{max} but not K_m for I^-.** *A* and *B*, both S43A and S581A mutants had reduced maximal rates of I^- transport compared with wild-type FLAGrNIS in transfected HEK293 cells. Initial velocities of I^- uptake were determined using varied concentrations of I^- (1–600 μM) with a final ^{125}I specific activity of 80 mCi/mmol. The data were plotted according to the Eadie-Hofstee plot. Each data point was performed in triplicate, and the mean ± S.D. is shown. The results are representative of three independent experiments. *Asterisks* denote a statistically significant difference in comparison with cells expressing wild-type FLAGrNIS ($p < 0.05$). *C*, the NIS V_{max} and K_m values for I^- are shown for phospho-defective S43A and S581A mutants as well as wild-type FLAGrNIS.

phosphorylated amino acid residues in rat NIS, Ser-43, Thr-49, and Ser-227, are conserved in human NIS. As the identified phosphorylated amino acid residue Ser-43 and its surrounding amino acid sequences are highly conserved between rat and human NIS, we next examined the role of phosphorylation status of Ser-43 in modulating human NIS functional activity and expression levels. Similarly, the hNIS S43A mutant had reduced RAIU activity, and the hNIS S43D mutant had RAIU activity comparable with that of wild-type FLAGhNIS (Fig. 5*A*). Both hNIS S43A and S43D mutants had total NIS protein levels (Fig. 5*B*) and cell surface NIS protein levels (Fig. 5*C*) comparable with those of wild-type FLAGhNIS.

Phospho-defective Mutant of either Ser-43 or Ser-581 Has Reduced Transport Rate of Iodide—Because the cell surface NIS level was not decreased in cells expressing S43A or S581A, we examined their kinetic properties of I^- uptake. As shown in Fig. 6, *A* and *B*, cells expressing S43A or S581A had reduced maximal rate of I^- transport (V_{max}) by 36 ± 11.7 and 59 ± 12.6%, respectively, compared with cells expressing wild-type FLAGrNIS. The finding that S43A or S581A had no apparent effect on K_m for I^- indicated that their reduced steady-state RAIU activity was not contributed by decreased NIS binding affinity for substrate I^- (Fig. 6*C*). Taken together, phosphorylation of Ser-43 and Ser-581 appears to increase NIS-mediated RAIU activity by increasing the velocity of iodide transport.

DISCUSSION

Phosphorylation can affect the functional activity, subcellular localization, and/or protein stability of various channels and transporters (10–18). Although it has been shown that NIS is a phosphorylated protein in FRTL-5 rat thyroid cells (2), no phosphorylated amino acid residues have yet been identified. In this study, we identified Ser-43, Thr-49, Ser-227, Thr-577, and Ser-581 as *in vivo* phosphorylated amino acid residues in rNIS expressed in heterologous HEK293 cells. We found that the velocity of iodide transport of rNIS is modulated by the phosphorylation status of Ser-43 and Ser-581 and that NIS protein stability may be modulated by the phosphorylation status of Thr-577. However, NIS cell surface trafficking was not affected by the phosphorylation status of these five amino acid residues. We have shown that NIS expression and functional activity could be modulated by post-translational modification through distinct mechanisms.

Based on current proposed topology, the intracellular domains of rNIS contain 28 serine, threonine, and tyrosine residues, of which Ser-43, Tyr-269, Thr-442, Thr-548, Ser-551, Ser-552, Thr-566, Thr-575, Thr-577, Ser-581, Thr-593, and Thr-605 are possibly phosphorylated as analyzed by phosphorylation prediction programs KinasePhos, NetPhos2.0, PredPhospho, and Prosite. In this study, we showed that the predicted phosphorylation residues Ser-43, Thr-577, and Ser-581 are indeed phosphorylated *in vivo*. The fact that Thr-49 and Ser-227 were not predicted to be phosphorylated by all four phosphorylation prediction programs underscores the importance of unbiased experimental approaches such as mass spectrometry to localize phosphorylation sites. It is difficult to conclude whether Tyr-269, Thr-442, Thr-548, Ser-551, Ser-552, Thr-566, Thr-575, Thr-593, and Thr-605 amino acid residues are not phosphorylated *in vivo* because of the transient nature of this post-translational modification. In addition, it is important to note that Ser-43, Thr-49, Ser-227, Thr-577, and Ser-581 were identified as phosphorylated amino acid residues under nonstimulated conditions. Thus, additional amino acid residues, such as those amino acid residues that were predicted to be phosphorylated, may be phosphorylated upon activation of various signaling.

Although the phosphorylation of Ser-227 in rNIS appears to be functionally silent, Ser-227 is nevertheless phosphorylated *in vivo*. It was surprising to have identified Ser-227 as a phosphorylated amino acid residue by LC-MS/MS analysis, as it is in close proximity to the experimentally determined *N*-linked glycosylation site Asn-225 (19). This indicates that Ser-227 is possibly located in the extracellular domains of rNIS. Phosphorylation of amino acid residues located in the extracellular regions of membrane proteins has been reported. Two tyrosine residues located in the extracellular domains of fibroblast growth factor receptor 1 were identified independently as phosphorylated residues by two different groups of investigators (20, 21). In addition, phosphorylation of extracellular domains of T-lymphocyte surface proteins was also reported (22). Although phosphorylation of extracellularly located amino acid residues is not unprecedented, it is nevertheless unusual. Alternatively, Ser-227 may be located in the intracellular domain, as conclusive topology of NIS has yet to be resolved by x-ray crystallography.

Molecular analyses of NIS missense mutations occurring in patients with congenital iodide transport defects have revealed not only the amino acid residues but also the underlying mechanisms that are critical for optimal NIS activity. It has been shown that substitution of glutamic acid at position 267 with any charged residue reduces NIS activity without decreasing NIS cell surface (23). Furthermore, the presence of an uncharged amino acid residue with a small side chain at position 395 (24), as well as the presence of a hydroxyl group at position 354 (25), is required for optimal NIS activity. Finally, De la Vieja *et al.* (26) recently reported that Asn-360, Asp-369, and the hydroxyl group containing residues Thr-351, Ser-353, Thr-354, Ser-356, and Thr-357 play key roles in Na^+ binding/translocation. In this study, we showed that substitution of phosphorylation residue Thr-49 with Ala, Asp, or Ser resulted in partial NIS activity of similar extent without affecting NIS protein levels. Thus, the structural constraint provided by the threonine residue at position 49, rather than its phosphorylation status, is important for NIS to achieve optimal activity.

The finding that T577A had reduced total protein levels, whereas T577D had total protein levels equivalent to those of wild-type NIS, suggests that the phosphorylation status of Thr-577 may affect NIS protein stability. However, we cannot exclude the possibility that a structural change of T577A targets it for degradation, which may not occur in the corresponding nonphosphorylated residue in wild-type NIS. Interestingly, during our initial proteomic analysis, we identified ubiquitin as a possible NIS-associated protein and later confirmed their association by co-immunoprecipitation studies (data not shown). Several studies have reported the role of phosphorylation as inhibitory to protein ubiquitination. Rolli-Derkinderen *et al.* (27) stated that phosphorylation of Ser-188 in RhoA prevented its ubiquitin-mediated proteasomal degradation. Moreover, it has been demonstrated that phospho-defective mutation of Bcl-2 at three amino acid residues rendered it susceptible to ubiquitin-dependent proteasomal degradation (28).

It is well established that phosphorylation can directly affect the activity of transporters and channels (10, 11, 13, 14, 29–31). In this study, we conclude that phosphorylation of NIS at both Ser-43 and Ser-581 residues is required for its optimal activity. In addition, kinetic analysis demonstrated that phosphorylation of these two sites does not affect the binding affinity for iodide, but rather the velocity of I^- transport. It would be most interesting to identify the kinases/phosphatases that modulate NIS phosphorylation status at these two residues. Using consensus motif programs GPS, KinasePhos, MotifScan, NetPhosK1.0, and PPSP, we have identified CK1, IPL1, and polo-like kinase as candidate kinases that may phosphorylate both Ser-43 and Ser-581 residues. However, CK2, G protein-coupled receptor kinase, phosphorylase kinase, protein kinase Cζ, cGMP-dependent protein kinase, and S6 protein kinase are predicted to phosphorylate Ser-43 but not Ser-581, whereas IκB kinase, MAPK kinase kinase, NIMA, and p21-activated kinase may possibly phosphorylate Ser-581 but not Ser-43. The roles of these candidate kinases in phosphorylation of Ser-43 or Ser-581

as well as in NIS activity need to be further explored. Alternatively, we are currently in the process of screening for kinases that modulate NIS functional activity using a small interfering RNA library targeting 719 kinases.

As the cellular context of various cells may be different, the sites of phosphorylation in NIS may also be different in heterologous HEK293 cells and endogenous NIS-expressing cells. As it is difficult to immunopurify sufficient amounts of endogenous NIS for mass spectrometry analysis, it would be desirable to generate phospho-site-specific antibodies to confirm that the corresponding sites are also phosphorylated in endogenous NIS. Interestingly, we reported previously that MEK inhibitor PD98059 decreased NIS activity by decreasing the velocity of iodide transport by a yet-to-be-identified mechanism (3). Accordingly, we examined whether the NIS S43D or S581D mutant would be resistant to PD98059 inhibition of NIS activity. However, both S43D and S581D remained sensitive to PD98059 inhibition of NIS activity (data not shown). We thus conclude that PD98059 does not appear to modulate NIS activity by altering the phosphorylation status of Ser-43 or Ser-581.

In summary, our study advances our knowledge of NIS modulation at the post-translational levels. We have identified Ser-43, Thr-49, Ser-227, Thr-577, and Ser-581 as *in vivo* phosphorylated amino acid residues in NIS and demonstrated their functional importance. Our findings indicate that NIS expression and activity can be modulated by phosphorylation at different amino acid residues. Accordingly, NIS expression and activity may be subjected to modulation by multiple signaling pathways involved in activation/inactivation of kinases/phosphatases. Indeed, NIS phosphorylation has been shown to be modulated by thyroid-stimulating hormone, which activates multiple signaling pathways in thyroid cells. Furthermore, inhibition of the MEK/MAPK signaling pathway, which is frequently activated in thyroid cancer, appears to increase NIS expression levels but decrease its activity. A better understanding of the cellular factors involved in controlling the phosphorylation status of NIS may lead to the identification of novel therapeutic targets for improved NIS-mediated radionuclide treatment of thyroid cancer.

Acknowledgment—We thank Dr. Tsung-Lin Liao for advice in mass spectrometry.

REFERENCES

1. Eskandari, S., Loo, D. D., Dai, G., Levy, O., Wright, E. M., and Carrasco, N. (1997) *J. Biol. Chem.* **272,** 27230–27238
2. Riedel, C., Levy, O., and Carrasco, N. (2001) *J. Biol. Chem.* **276,** 21458–21463
3. Vadysirisack, D. D., Venkateswaran, A., Zhang, Z., and Jhiang, S. M. (2007) *Endocr.-Relat. Cancer* **2,** 421–432
4. Castro, M. R., Bergert, E. R., Goellner, J. R., Hay, I. D., and Morris, J. C. (2001) *J. Clin. Endocrinol. Metab.* **86,** 5627–5632
5. Tonacchera, M., Viacava, P., Agretti, P. de Marco, G., Perri, A., di Cosmo, C., de Servi, M., Miccoli, P., Lippi, F., Naccarato, A. G., Pinchera, A., Chiovato, L., and Vitti, P. (2002) *J. Clin. Endocrinol. Metab.* **87,** 352–357
6. Zhang, Z., Liu, Y. Y., and Jhiang, S. M. (2005) *J. Clin. Endocrinol. Metab.* **90,** 6131–6140
7. Olsen, J. V., Blagoey, B., Gnad, F., Macek, B., Kumar, C., Mortensen, P., and Mann, M. (2006) *Cell* **127,** 635–648
8. Wu, S. L., Kim, J., Bandle, R. W., Liotta, L., Petricoin, E., and Karger, B. L. (2006) *Mol. Cell. Proteomics* **5,** 1610–1627
9. Smanik, P. A., Liu, Q., Furminger, T. L., Ryu, K., Xing, S., Mazzaferri, E. L., and Jhiang, S. M. (1996) *Biochem. Biophys. Res. Commun.* **226,** 339–345
10. Han, X., Budreau, A. M., and Chesney, R. W. (1999) *J. Am. Soc. Nephrol.* **10,** 1874–1879
11. Surti, T. S., Huang, L., Jan, Y. N., Jan, L. Y., and Cooper, E. C. (2005) *Proc. Natl. Acad. Sci. U. S. A.* **102,** 17828–17833
12. Ren, Y., Barnwell, L. F., Alexander, J. C., Lubin, F. D., Adelman, J. P., Pfaffinger, P. J., Schrader, L. A., and Anderson, A. E. (2006) *J. Biol. Chem.* **281,** 11769–11779
13. Roosbeek, S., Peelman, F., Verhee, A., Labeur, C., Caster, H., Lensink, M. F., Cirulli, C., Grooten, J., Cochet, C., Vanderkerckhove, J., Amoresano, A., Chimini, G., Tavernier, J., and Rosseneu, M. (2004) *J. Biol. Chem.* **279,** 37779–37788
14. Park, K. S., Mohapatra, D. P., Misonou, H., and Trimmer, J. S. (2006) *Science* **313,** 976–979
15. Jayanthi, L. D., Annamalai, B., Samuvel, D. J., Gether, U., and Ramamoorthy, S. (2006) *J. Biol. Chem.* **281,** 23326–23340
16. Law, R. M., Stafford, A., and Quick, M. W. (2000) *J. Biol. Chem.* **275,** 23986–23991
17. Martinez, L. O., Agerholm-Larsen, B., Wang, B., Chen, W., and Tall, A. R. (2003) *J. Biol. Chem.* **278,** 37368–37374
18. Huff, R. A., Vaughan, R. A., Kuhar, M. J., and Uhl, G. R. (1997) *J. Neurochem.* **68,** 225–232
19. Levy, O., De la Vieja, A., Ginter, C. S., Riedel, C., Dai, G., and Carrasco, N. (1998) *J. Biol. Chem.* **273,** 22657–22663
20. Hou, J., McKeehan, K., Kan, M., Carr, S. A., Huddleston, M. J., Crabb, J. W., and KcKeehan, W. L. (1993) *Protein Sci.* **2,** 86–92
21. Hinsby, A. M., Olsen, J. V., Bennett, K. L., and Mann, M. (2003) *Mol. Cell. Proteomics* **1,** 29–36
22. Apasov, S. G., Smith, P. T., Jelonek, M. T., Marguilies, D. H., and Sitkovsky, M. V. (1996) *J. Biol. Chem.* **271,** 25677–25683
23. De la Vieja, A., Ginter, C. S., and Carrasco, N. (2004) *J. Cell Sci.* **117,** 677–687
24. Dohan, O., Gavrielides, M. V., Ginter, C., Amzel, L. M., and Carrasco, N. (2002) *Mol. Endocrinol.* **16,** 1893–1902
25. Levy, O., Ginter, C. S., De la Vieja, A., Levy, D., and Carrasco, N. (1998) *FEBS Lett.* **429,** 36–40
26. De la Vieja, A., Reed, M. D., Ginter, C. S., and Carrasco, N. (2007) *J. Biol. Chem.* **282,** 25290–25298
27. Rolli-Derkinderen, M., Sauzeau, V., Boyer, L., Lemichez, E., Baron, C., Henrion, D., Loirand, G., and Pacaud, P. (2005) *Circ. Res.* **11,** 1152–1160
28. Breitschopf, K., Haendeler, J., Malchow, P., Zeiher, A. M., and Dimmeler, S. (2000) *Mol. Cell. Biol.* **20,** 1886–1896
29. Glavy, J. S., Wu, S. M., Wang, P. J., Orr, G. A., and Wolkoff, A. W. (2000) *J. Biol. Chem.* **275,** 1479–1484
30. Lee, T. S., Karl, R., Moosmang, S., Lenhardt, P., Klugbauer, N., Hofmann, F., Kleppisch, T., and Welling, A. (2006) *J. Biol. Chem.* **281,** 25560–25567
31. Xu, Z. C., Yang, Y., and Hebert, S. C. (1996) *J. Biol. Chem.* **271,** 9313–9319